# Intravascular ultrasound appearance of scattered necrotic core as an index for deterioration of coronary flow during intervention in acute coronary syndrome



doi: 10.1007/s00380-011-0175-8

*Heart and Vessels*

**Category:** Original Articles

**HEVE-D-10-00332R2**

# Intravascular Ultrasound Appearance of Scattered Necrotic Core as an Index for Deterioration of Coronary Flow During Intervention in Acute Coronary Syndrome

Kenji Sakata, MD,[1]* Masa-aki Kawashiri, MD, [1] Hidekazu Ino, MD, [1]

Takao Matsubara, MD,[2] Yoshihide Uno, MD, [2] Toshihiko Yasuda, MD, [2]

Kenji Miwa, MD, [2] Honin Kanaya, MD, [2] and Masakazu Yamagishi, MD, FACC[1]

[1]Division of Cardiovascular Medicine, Kanazawa University Graduate School of Medicine, Kanazawa, and [2]Division of Cardiology, Ishikawa Prefectural Central Hospital, Kanazawa, Japan.

**Short title:** Plaque distribution and coronary flow deterioration

*__Corresponding Author:__

Kenji Sakata, MD

Division of Cardiovascular Medicine,

Kanazawa University Graduate School of Medicine

13-1 Takara-machi, Kanazawa, Ishikawa 920-8640, Japan

Telephone: +81-76-265-2254, Fax: +81-76-234-4210

E-mail: kenjis@yu.incl.ne.jp

**Abstract**

**Background:** In acute coronary syndrome (ACS) patients with deterioration of coronary flow during percutaneous coronary intervention (PCI), a scattered necrotic core pattern (SNC) is observed by intravascular ultrasound Virtual Histology (VH-IVUS). The purpose of this study was to evaluate the impact of SNC on deterioration of coronary flow during PCI in ACS.

**Methods:** A total of 38 ACS patients were imaged using VH-IVUS before PCI. In addition to conventional definitions of thin-cap fibroatheroma by VH-IVUS (ID-TCFA), the SNC was defined as necrotic core foci with a maximum diameter of <14 pixels on a 400 × 400 VH-IVUS image in the presence of >50% plaque burden except in the ID-TCFA frame.

**Results:** Patients were divided into deterioration of coronary flow group (n = 15) and normal-reflow group (n = 23). The incidence of residual thrombus and plaque rupture, the external elastic membrane, plaque and fibrous volumes, the incidence of ID-TCFA and the average number of SNC per frame was significantly greater in deterioration of coronary flow group than in normal-reflow group ($P$ <0.05 all parameters). Multivariate analysis revealed that the average number of SNC per frame was independently associated with deterioration of coronary flow in ACS patients (odds ratio 1.18, $P$ <0.05).

**Conclusions:** Increased number of SNC is associated with deterioration of coronary flow during PCI in ACS patients.

**Key Words:** acute coronary syndrome (ACS), intravascular ultrasound, percutaneous coronary intervention (PCI)

## Introduction

In the era of primary intervention for acute coronary syndrome (ACS), several investigators have documented that the slow flow phenomenon during or after primary coronary intervention (PCI) results in reduced left ventricular ejection fraction, left ventricular remodeling, and poor clinical outcomes[1]. Indeed, recent intravascular ultrasound (IVUS) studies have shown that decreased plaque volume, as a result of mechanical dilation or disruption, contributes to the mechanism of embolization[2]. Therefore, accurately identifying lesion characteristics and plaque components at high risk of causing slow flow during an interventional procedure is of crucial importance[3].

As a qualitative assessment, previous studies have suggested that the presence of a lipid core, plaque rupture of vulnerable lesions and thrombus formation are all associated with the no-reflow phenomenon[4, 5]. Furthermore, pathological analysis of the aspirates taken at the time of the no-reflow phenomenon has detected not only thrombus formation, but also plaque components, including foam-shaped macrophages, aggregated platelets, and cholesterol crystals[6]. Virtual Histology (VH)-IVUS uses spectral analysis of the radiofrequency ultrasound backscatter signals which allows the identification of four different types of atherosclerotic plaque components: fibrous, fibrofatty, dense calcium, and necrotic core, and provides some important information on lesion characteristics and other plaque components[7]. A recent VH-IVUS study suggested that heterogeneity of plaque components, such as fibrous and fibrofatty rich plaque, was associated with no-reflow phenomenon[8]. VH-IVUS images of vulnerable plaque at culprit lesions in a saphenous vein graft showed the presence of fibrofatty[9] and fibrofatty plaque with scattered necrotic core (SNC)[10]. Furthermore, we have often observed SNC by VH-IVUS in ACS patients with deterioration of coronary flow during

PCI. Accordingly, we hypothesized that the identification of SNC by VH-IVUS would be associated with the deterioration of coronary flow during an interventional procedure in patients with ACS. The aim of this study was to investigate the relationship between the pre-interventional lesion characteristics and incidence of deterioration of coronary flow during PCI in ACS patients, using VH-IVUS methodology.

## Methods

### Patients

Forty-nine consecutive patients with ACS were enrolled in the study. The patients had either acute myocardial infarction (AMI) within 24 hours of onset or unstable angina of Braunwald class IIIB (i.e. angina at rest within 48 hours, with no creatine kinase-MB elevation). The diagnosis of AMI was determined by the presence of >30 minutes of continuous chest pain, ST-segment elevation >2.0 mm on at least 2 contiguous electrocardiogram leads, >3-fold increase in serum creatine kinase levels, and thrombolysis in myocardial infarction (TIMI) flow grade 0, 1, or 2 at the time of the initial emergency coronary angiography[11]. We excluded patients with a previous myocardial infarction of the target vessel, bypass failure, subacute thrombosis or restenosis after PCI, chronic total occlusion, and atrial fibrillation. Patients in whom adequate IVUS images could not be obtained were also excluded. A glycoprotein IIb/IIIa inhibitor was not used in this study, because of its nonavailability in the country where this study was performed (Japan). Written informed consent was obtained from all subjects in accordance with the guidelines of the Bioethical Committee on Medical Researches, Ishikawa Prefectural Central Hospital.

**PCI procedure and IVUS imaging protocol**

Coronary angiography was performed via the femoral or radial approach. All patients received an intravenous bolus injection of 3,000 IU of heparin and intracoronary isosorbide dinitrate (2 mg) before angiography. Before PCI, an additional 5,000 IU of heparin was administered and a conventional 0.014-inch guidewire was advanced beyond the target lesion. If thrombi had been detected angiographically or the lesion presented with a total occlusion, an aspiration catheter was advanced over the guidewire and a thrombectomy was performed. After adjunctive thrombectomy, TIMI II or III coronary flow was confirmed angiographically. A 20-MHz, 3.2-F phased-array IVUS catheter (Eagle Eye Gold, Volcano Corp, Rancho Cordova, CA) was carefully advanced to a position distal to the lesion, and was then pulled back at a rate of 0.5 mm/s from the distal to the proximal part, using an auto-motorized pullback system. Balloon dilatation or stent implantation was performed after IVUS examination.

**Angiographical analysis**

The offline quantitative coronary angiography analyses were performed by 2 experienced observers who were unaware of the IVUS measurements using the automated edge detection system (Anchor, Siemens or Cardiovascular Measurement System, Goodman). From the quantitative coronary angiography images, the minimal lumen diameter, diameter stenosis and length of the stenosis were calculated. The corrected TIMI frame count, which is a quantitative parameter of reperfusion epicardial flow, after thrombectomy and immediately after mechanical dilation (e.g. balloon inflation, stent deployment), was estimated in the infarct-related artery as previously reported[12]. We defined deterioration of coronary flow during PCI as an increase in the

corrected TIMI frame count after mechanical dilation compared with corrected TIMI frame count after thrombectomy, and without any evidence of dissection, severe stenosis, and vasospasm.

**Grayscale and VH-IVUS data analysis**

Serial IVUS images were digitized and stored on the hard disk of the IVUS console (IVG3, Volcano Corp, Rancho Cordova, CA) for off-line analysis. Quantitative volumetric grayscale and VH-IVUS analysis were performed across the entire lesion segment, and cross-sectional analysis was performed at minimal lumen sites. Qualitative assessment and quantitative measurements were performed as previously reported[13]. The culprit lesion was defined as the site of the smallest lumen, and the reference segments were the most normal-looking cross-sectional area (CSA) within 5 mm proximal and distal to the lesion. Morphometric parameters of external elastic membrane (EEM) CSA and lumen CSA were measured at the lesion and the reference site. Plaque and media CSA were calculated as EEM CSA minus lumen CSA, and plaque burden was calculated as plaque and media CSA divided by EEM CSA × 100. Remodeling index was calculated as the EEM CSA at the minimum lumen diameter divided by the proximal reference EEM CSA. Positive remodeling was defined as remodeling index >1.0. Thrombus formation was defined as a distinct hypoechoic mass, brightly speckled plaque, the presence of channels into the plaque, evacuated plaque cavity and an intraluminal mobile mass. A lipid pool-like image was defined as a pooling of low echogenic material that was covered by a thin, high-echogenic layer. Ruptured plaque was defined as plaque ulceration with a torn fibrous cap. Spotty calcification was defined as bright echoes in the vessel wall with an arc ≤90° with

acoustic shadowing. The frequency of thrombus, ruptured plaque, lipid pool-like image and spotty calcification was assessed visually. In VH-IVUS analysis, the volumetric reconstruction of the plaques was performed off-line using VH software (IVG3, Volcano Corp, Rancho Cordova, CA) using the trapezoidal method. For each segment, EEM and lumen borders were identified using automatic edge detection and manually corrected when necessary. Areas or volumes of the four different VH-IVUS plaque components were automatically calculated for every recorded frame and for the entire imaged segment. On the reconstructed color-coded tissue map, fibrous areas were marked in green, fibrofatty in yellow, dense calcium in white and necrotic core in red. The four VH-IVUS plaque components were reported in absolute amounts and as a percentage of plaque area or volume.

On the other hand, thin-cap fibroatheroma (TCFA) is one type of vulnerable plaque morphology, and the rupture of TCFA with subsequent thrombus formation is accepted as the most frequent cause of ACS. The quantitative definition of TCFA by VH-IVUS (VH-IVUS defined TCFA; ID-TCFA) was plaque burden >50% and a confluent necrotic core extending >14 pixels along the circumference of the lumen on a 400 × 400 pixel VH-IVUS image; the final assignment of the ID-TCFA phenotype required identification of ID-TCFA on 3 consecutive frames, with or without confluent dense calcium, by using an automated pixel detection algorithm based on a histopathologic classification system[14]. On the basis of this definition, we defined SNC, which represents the ruptured TCFA associated with deterioration of coronary flow during intervention, as a necrotic core foci with a maximum diameter of <14 pixels on a 400 × 400 VH-IVUS image in the presence of >50% plaque burden except in the ID-TCFA frame (Fig. 1). SNC and ID-TCFA was analyzed using NIH ImageJ version

1.42q software (http://rsbweb.nih.gov/ij/) for the delineation and quantification of cross-sectional areas of necrotic core foci in each frame. Subsequently, the proportion of SNC in the “all necrotic core area” and the total number of SNC at the minimum lumen area site were calculated, and the proportion of ID-TCFA, the total number of SCN, the maximum number of SNC, the proportion of SNC in the “all necrotic core volume”, and the average number of SNC/frame by dividing the total number of SNC by the total number of frames within the segment, were calculated.

**Statistical analysis**

Values are expressed as mean ± standard deviation or proportions. Differences between groups were analyzed by the Student’s unpaired t-test. Categorical data were compared by Chi-square analysis. Correlation was assessed by linear regression analysis and Pearson’s correlation coefficient. Univariate and multivariate logistic regression analyses were used to identify predictors of the deterioration of coronary flow during PCI procedure. Univariate predictors with *P* value <0.1 were entered into the multivariate model. A *P* value <0.05 was considered statistically significant. Stat View 5.0 (SAS Institute, Cary, NC) was used for data analysis.

**Results**

A conventional wire was successfully positioned beyond the target lesions in all 49 ACS patients. However, 11 cases had to be excluded from the analysis for the following reasons: the IVUS catheter could not be advanced beyond the calcified stenosis (3 cases); inadequate IVUS images (7 cases); and the wire dissection occurred before the IVUS catheter could be advanced beyond the stenosis (1 case). Therefore, 38

cases (30 males, 8 females; mean age 65.9 ± 13.6 years) were included in the final analysis. Patients were divided into a coronary flow deterioration group (n = 15) and a normal reflow group (n = 23) as determined by corrected TIMI frame count.

Baseline characteristics, angiographical and PCI procedure analysis are listed in Table 1 and were not significantly different between the two groups with the exceptions of age (normal reflow group patients were significantly older than slow flow group patients) and post-interventional corrected TIMI frame count, which was statistically greater in the coronary flow deterioration group as befitted the classification. Conventional IVUS analysis is summarized in Table 2. The EEM CSA, plaque & media CSA and lumen CSA did not differ significantly at minimal lumen site. In contrast, the EEM volume was significantly greater in the coronary flow deterioration group than in the normal reflow group ($P$ = 0.0292), but there was no statistical difference in the lumen volume ($P$ = 0.39). Consequently, plaque & media volume was larger in the coronary flow deterioration group than in the normal reflow group ($P$ = 0.0494). The presence of residual thrombus and ruptured plaque occurred more frequently in the coronary flow deterioration group than in the normal reflow group ($P$ = 0.0096, $P$ = 0.0011, respectively). However, there were no differences between the two groups in the lipid pool-like image, positive remodeling and spotty calcification.

We then analyzed plaque composition by VH-IVUS (Table 3). At the minimum lumen site, the absolute fibrous plaque area was significantly greater in the coronary flow deterioration group compared with normal flow group. Within the entire culprit lesions, the absolute fibrous volume was significantly greater in coronary flow deterioration group than in normal reflow group ($P$ = 0.0318). Additionally, we investigated the VH-IVUS-derived plaque distribution analysis. At the minimum lumen

site, the number of SNC and the proportion of SNC/necrotic core were significantly greater in coronary flow deterioration group than normal flow group ($P$ = 0.0004 and $P$ = 0.0295, respectively). Within the entire culprit lesion, the incidence of ID-TCFA, the average number of SNC, and maximum number of SNC were significantly greater in coronary flow deterioration group than in normal reflow group. However, the proportion of SNC in the all NC volume did not differ between the two groups.

Multiple logistic regression analysis between patients with and without deterioration of coronary flow, including age, EEM volume, absolute fibrous volume, residual thrombus, plaque rupture, the incidence of ID-TCFA, and the average number of SNC/frame as covariates, showed that the average number of SNC/frame (odds ratio 1.182, 95% confidence interval 1.023 to 1.366, $P$ = 0.0229) was the most effective predictor of coronary flow deterioration during PCI (Table 4).

In order to evaluate the relationship between the severity of coronary flow deterioration and plaque distribution, a linear regression analysis was performed (Fig. 2). CTFC after mechanical dilation, which means the degree of deterioration of coronary flow during PCI, correlated strongly with the average number of SNC/frame (R = 0.71, $P$ <0.0001), however, CTFC after mechanical dilation did not correlate with the incidence of ID-TCFA (R = 0.26, $P$ = 0.1).

We identified some ACS patients with coronary flow deterioration after intervention whose grayscale IVUS findings at the target lesion were a mixture of soft plaque and thrombi, and whose VH-IVUS findings from the target lesion showed SNC foci diffusely distributed throughout the plaque area, generally in plaque comprising mainly a mixture of fibrous and fibrofatty components, as shown in Fig. 3. Moreover, microscopic findings from materials collected by thrombectomy in some patients with

coronary flow deterioration with SNC by VH-IVUS were mixed thrombi and cholesterol clefts, which are considered as major causes of this phenomenon (Fig. 3). Fig. 4 shows VH-IVUS color-coded images and corrected TIMI frame count after mechanical dilatation from 3 representative cases.

**Discussion**

The present study demonstrated that the incidence of residual thrombus, plaque rupture, EEM volume, fibrous volume, the incidence of ID-TCFA, and the average number of SNC/frame were significantly greater in patients with coronary flow deterioration than in those with normal flow. Notably, in our ACS patients, the average number of SNC/frame was the most effective predictor of the occurrence of coronary flow deterioration during the intervention procedure, and there was a significant relationship between the average number of SNC within lesions on VH-IVUS and the degree of coronary flow deterioration.

Recent VH-IVUS studies have demonstrated that, as a qualitative assessment, necrotic core component and necrotic core volume predict the risk of distal embolization after primary stent deployment in patients with ST-segment elevation myocardial infarction[15]. Bae et al. reported that fibrofatty volume was the only independent factor for slow flow during PCI in AMI patients[16]. In contrast to the previous studies, we found that fibrous volume was significantly greater in the coronary flow deterioration group than in the normal flow group. Therefore, the predictor of coronary flow deterioration by VH-IVUS in ACS patients remains controversial. Discrepancy between these findings might be explained by the existence of a thrombus at the analyzed lesions. In general, most patients with ACS are more likely to have

ruptured plaques with a superimposed thrombus at the target lesion[17]. The composition of thrombus tissue in ACS patients is very heterogeneous, because it depends on age of the thrombus[18]. Moreover, a thrombus cannot be identified using VH-IVUS because of a lack of histological validation. Nasu et al. reported that intramural thrombi were mistakenly colored as fibrous or fibrofatty tissue by VH-IVUS[19]. From the pathologic classification, an organized thrombus shows ingrown smooth muscle cells with or without depositions of connective tissue and capillary vessel growth, which is similar to fibrous plaque. Thus, because an organized thrombus could often have been included in the analysis area of VH-IVUS in this study, plaque composition of a target lesion obtained by VH-IVUS was in contradiction with histopathological data, with more fibrous tissue volume that could result in a lower percentage necrotic core volume in the coronary flow deterioration group compared with previous reports[15, 20]. From these findings, it is possible that the difference between the various findings using VH-IVUS is a reflection of the presence of a thrombus and its relative age. Therefore, it is difficult to predict the deterioration of coronary flow during PCI in ACS by using the proportion of conventional 4 types of plaque tissue components obtained from VH-IVUS.

In the present study, according to both VH-IVUS findings and pathological findings, we demonstrated that the identification of SNC by VH-IVUS would be associated with ruptured plaque with thrombus formation, which caused the deterioration of coronary flow. Furthermore, the most effective predictor of the deterioration of coronary flow was not fibrous volume but the average number of SNC/frame, which in turn may be influenced by the distribution of plaque components, rather than their relative proportions. On the other hand, a previous VH-IVUS study suggested that post-stenting no-reflow was associated with ID-TCFA in ACS patients[20].

In the present study, although ID-TCFA was also observed more frequently in the coronary flow deterioration group than in the normal reflow group, the average number of SNC/frame was the most effective predictor of the occurrence of deterioration of coronary flow during the intervention procedure rather than the incidence of ID-TCFA. From these results, once vulnerable plaque is ruptured in ACS patients, it is difficult to detect ID-TCFA because intramural thrombi covered the necrotic core along the circumference of the lumen at the culprit lesion. Therefore, it is possible that the incidence of ID-TCFA in ACS may depend on the amount of residual intramural thrombus. However, the relationship between the presence of SNC and the occurrence of deterioration of coronary flow during the intervention procedure is still unclear. In humans, the no-reflow phenomenon has a multifactorial pathogenesis. Angioplasty-induced distal coronary embolization of plaque and thrombus may compound the vascular obstruction. Furthermore an inflammatory response induced by neutrophils and platelets occurs at the time of reperfusion may exacerbate this process, which leads to further myocardial ischemia and cell death, resulting from a longer reperfusion time[21, 22]. As the necrotic core components contain fragile tissues, such as lipid deposition with foam cells, intramural bleeding, and cholesterol crystals, they can be easily liberated as small emboli by mechanical fragmentation during coronary stenting. Pathological analysis of the aspirates at the time of no-reflow phenomenon have detected not only thrombi but also plaque components including foam-shaped macrophages, aggregated platelets, and cholesterol crystals[6], of which the latter might be identified by VH-IVUS as necrotic core. From these findings, SNC might be associated with the mixture of the thrombi and plaque component, such as cholesterol crystals. Moreover, the inflammatory response induced by aggregated platelets, which causes reperfusion injury,

may be associated with SNC. Further pathological studies are needed to clarify the relationship between SNC and the occurrence of coronary flow deterioration.

**Study limitations**

Some limitations of the study should be acknowledged. First, the accuracy of volumetric analysis by a motorized pull-back system Eagle Eye™ IVUS catheter may be lower than a mechanical rotational catheter[23], because this motorized catheter pulls the IVUS catheter itself. However, in the present study, the IVUS catheter was pulled back smoothly, because most of the target lesion was soft after aspiration of the thrombus and plaque in patients with ACS, compared with tight and calcified stenosis in patients with stable angina pectoris. Therefore, we feel that the accuracy of volumetric analysis by an Eagle Eye™ IVUS catheter is acceptable to a certain extent in the clinical setting of ACS. Second, thrombus aspiration prior to IVUS was not performed for all patients, which may have biased the results. Third, as only 5 patients (13%) had final TIMI flow grade 2 or less (no-reflow group), it was difficult to compare no-reflow group with normal-reflow group in this study. No-reflow phenomenon has been reported to be predictive for poor clinical outcomes, whilst deterioration of coronary flow as defined in this study has not. Further studies are needed to clarify the relationship between deterioration of coronary flow and clinical outcomes. Fourth, this study is limited by the relatively small number of patients. However, SNC remained predictive of coronary flow deterioration during PCI despite the size of the patient sample. Larger studies will be necessary to determine whether SNC can predict clinical outcomes.

**Conclusions**

In addition to conventional indices such as EEM volume, increased SNC number by VH-IVUS is highly associated with corrected TIMI frame count after intervention. Approaches to preventing possible coronary flow deterioration in ACS patients who exhibit increased SNC number by VH-IVUS require further study.

**References**

1. Morishima I, Sone T, Okumura K, Tsuboi H, Kondo J, Mukawa H, Matsui H, Toki Y, Ito T, Hayakawa T (2000) Angiographic no-reflow phenomenon as a predictor of adverse long-term outcome in patients treated with percutaneous transluminal coronary angioplasty for first acute myocardial infarction. J Am Coll Cardiol 36:1202-1209

2. Sato H, Iida H, Tanaka A, Tanaka H, Shimodouzono S, Uchida E, Kawarabayashi T, Yoshikawa J (2004) The decrease of plaque volume during percutaneous coronary intervention has a negative impact on coronary flow in acute myocardial infarction: a major role of percutaneous coronary intervention-induced embolization. J Am Coll Cardiol 44:300-304

3. Harigaya H, Motoyama S, Sarai M, Inoue K, Hara T, Okumura M, Naruse H, Ishii J, Hishida H, Ozaki Y (2010) Prediction of the no-reflow phenomenon during percutaneous coronary intervention using coronary computed tomography angiography. Heart Vessels Advance Access published on 6 November 2010. doi: 10.1007/s00380-010-0059-3

4. Iijima R, Shinji H, Ikeda N, Itaya H, Makino K, Funatsu A, Yokouchi I, Komatsu H, Ito N, Nuruki H, Nakajima R, Nakamura M (2006) Comparison of coronary arterial finding by intravascular ultrasound in patients with "transient no-reflow" versus "reflow" during percutaneous coronary intervention in acute coronary syndrome. Am J Cardiol 97:29-33

5. Kusama I, Hibi K, Kosuge M, Nozawa N, Ozaki H, Yano H, Sumita S, Tsukahara K, Okuda J, Ebina T, Umemura S, Kimura K (2007) Impact of plaque rupture on infarct size in ST-segment elevation anterior acute myocardial infarction. J

Am Coll Cardiol 50:1230-1237

6. Kotani J, Nanto S, Mintz GS, Kitakaze M, Ohara T, Morozumi T, Nagata S, Hori M (2002) Plaque gruel of atheromatous coronary lesion may contribute to the no-reflow phenomenon in patients with acute coronary syndrome. Circulation 106:1672-1677

7. Nair A, Kuban BD, Tuzcu EM, Schoenhagen P, Nissen SE, Vince DG (2002) Coronary plaque classification with intravascular ultrasound radiofrequency data analysis. Circulation 106:2200-2206

8. Nakamura T, Kubo N, Ako J, Momomura S (2007) Angiographic no-reflow phenomenon and plaque characteristics by virtual histology intravascular ultrasound in patients with acute myocardial infarction. J Interv Cardiol 20:335-339

9. Jim MH, Hau WK, Ko RL, Siu CW, Ho HH, Yiu KH, Lau CP, Chow WH (2010) Virtual histology by intravascular ultrasound study on degenerative aortocoronary saphenous vein grafts. Heart Vessels 25:175-181

10. Komatsu S, Omori Y, Murakawa T, Hirayama A, Ueda Y, Oyabu J, Fujisawa Y, Ogasawara N, Higashide T, Shimizu T, Kodama K (2007) Detection of saphenous vein graft by multidetector row computed tomography and composition with gray-scale/virtual histology intravascular ultrasound. Int J Cardiol 114:111-113

11. The TIMI IIIB Investigators (1994) Effects of tissue plasminogen activator and a comparison of early invasive and conservative strategies in unstable angina and non-Q-wave myocardial infarction. Results of the TIMI IIIB Trial. Thrombolysis in Myocardial Ischemia. Circulation 89:1545-1556

12. Gibson CM, Cannon CP, Daley WL, Dodge JT Jr, Alexander B Jr, Marble SJ, McCabe CH, Raymond L, Fortin T, Poole WK, Braunwald E (1996) TIMI frame count:

a quantitative method of assessing coronary artery flow. Circulation 93:879-888

13. Mintz GS, Nissen SE, Anderson WD, Bailey SR, Erbel R, Fitzgerald PJ, Pinto FJ, Rosenfield K, Siegel RJ, Tuzcu EM, Yock PG (2001) American College of Cardiology Clinical Expert Consensus Document on Standards for Acquisition, Measurement and Reporting of Intravascular Ultrasound Studies (IVUS). A report of the American College of Cardiology Task Force on Clinical Expert Consensus Documents. J Am Coll Cardiol 37:1478-1492

14. Lindsey JB, House JA, Kennedy KF, Marso SP (2009) Diabetes duration is associated with increased thin-cap fibroatheroma detected by intravascular ultrasound with virtual histology. Circ Cardiovasc Interv 2:543-548

15. Kawaguchi R, Oshima S, Jingu M, Tsurugaya H, Toyama T, Hoshizaki H, Taniguchi K (2007) Usefulness of virtual histology intravascular ultrasound to predict distal embolization for ST-segment elevation myocardial infarction. J Am Coll Cardiol 50:1641-1646

16. Bae JH, Kwon TG, Hyun DW, Rihal CS, Lerman A (2008) Predictors of slow flow during primary percutaneous coronary intervention: an intravascular ultrasound-virtual histology study. Heart 94:1559-1564

17. Hong MK, Mintz GS, Lee CW, Kim YH, Lee SW, Song JM, Han KH, Kang DH, Song JK, Kim JJ, Park SW, Park SJ (2004) Comparison of coronary plaque rupture between stable angina and acute myocardial infarction: a three-vessel intravascular ultrasound study in 235 patients. Circulation 110:928-933

18. Rittersma SZ, van der Wal AC, Koch KT, Piek JJ, Henriques JP, Mulder KJ, Ploegmakers JP, Meesterman M, de Winter RJ (2005) Plaque instability frequently occurs days or weeks before occlusive coronary thrombosis: a pathological

thrombectomy study in primary percutaneous coronary intervention. Circulation 111:1160-1165.

19. Nasu K, Tsuchikane E, Katoh O, Vince DG, Margolis PM, Virmani R, Surmely JF, Ehara M, Kinoshita Y, Fujita H, Kimura M, Asakura K, Asakura Y, Matsubara T, Terashima M, Suzuki T (2008) Impact of intramural thrombus in coronary arteries on the accuracy of tissue characterization by in vivo intravascular ultrasound radiofrequency data analysis. Am J Cardiol 101:1079-1083

20. Hong YJ, Jeong MH, Choi YH, Ko JS, Lee MG, Kang WY, Lee SE, Kim SH, Park KH, Sim DS, Yoon NS, Youn HJ, Kim KH, Park HW, Kim JH, Ahn Y, Cho JG, Park JC, Kang JC (2009) Impact of plaque components on no-reflow phenomenon after stent deployment in patients with acute coronary syndrome: a virtual histology-intravascular ultrasound analysis. Eur Heart J Advance Access published on 19 February 2009. doi:10.1093/ eurheartj/ehp034

21. Jaffe R, Charron T, Puley G, Dick A, Strauss BH (2008) Microvascular obstruction and the no-reflow phenomenon after percutaneous coronary intervention. Circulation 117:3152-3156

22. Niccoli G, Burzotta F, Galiuto L, Crea F (2009) Myocardial no-reflow in humans. J Am Coll Cardiol 54:281-292

23. Tanaka K, Carlier SG, Mintz GS, Sano K, Liu X, Fujii K, de Ribamar Costa J Jr, Lui J, Moses JW, Stone GW, Leon MB (2007) The accuracy of length measurements using different intravascular ultrasound motorized transducer pullback systems. Int J Cardiovasc Imaging 23:733-738

**Figure Legends**

**Fig. 1. An example of selective quantification of the scattered necrotic core**

**(A)** A conventional grayscale IVUS cross-sectional image at the target lesion. **(B)** Corresponding image using VH-IVUS. VH-IVUS shows plaque burden of 84%, %fibrous (green) of 63%, %fibrofatty (light green) of 23%, %necrotic core (red) of 13% and %dense calcium (white) of 1%. **(C)** Each necrotic core area is selectively delineated. **(D)** Total number of necrotic core foci and each necrotic core area are automatically calculated by software. In this frame, the total number of necrotic cores is 173 and the total number of scattered necrotic core is 90.

**Fig. 2. Correlation between corrected TIMI frame count after mechanical dilation and plaque distribution**

Following mechanical dilation, there were significant correlations between corrected TIMI frame count and the average number of scatter necrotic core/frame **(A)**, the incidence of VH-IVUS defined thin-cap fibroatheroma (ID-TCFA), however, did not correlate with corrected TIMI frame count after mechanical dilation **(B)**.

**Fig. 3. Microscopic findings from materials collected by thrombectomy in a patient with deterioration of coronary flow**

**(A)** Microscopic findings from materials collected by thrombectomy in a patient with slow flow were mixed thrombi (left) and cholesterol clefts (right). **(B)** Images of grayscale IVUS (upper) and VH-IVUS (lower). Grayscale IVUS findings at the target lesion were a mixture of soft plaque and thrombi, and VH-IVUS findings from the

target lesion were a scattered necrotic core pattern generally in plaque comprising mainly a mixture of fibrous and fibrofatty components.

**Fig. 4. Typical VH-IVUS images with or without coronary deterioration during PCI**

Typical VH-IVUS images without coronary deterioration **(A and B)** and with coronary deterioration during PCI **(C)**. **(A)** The total number of scattered necrotic core is 10. **(B)** The total number of scattered necrotic core is 15. **(C)** The total number of scattered necrotic core is 90.

Fig. 1

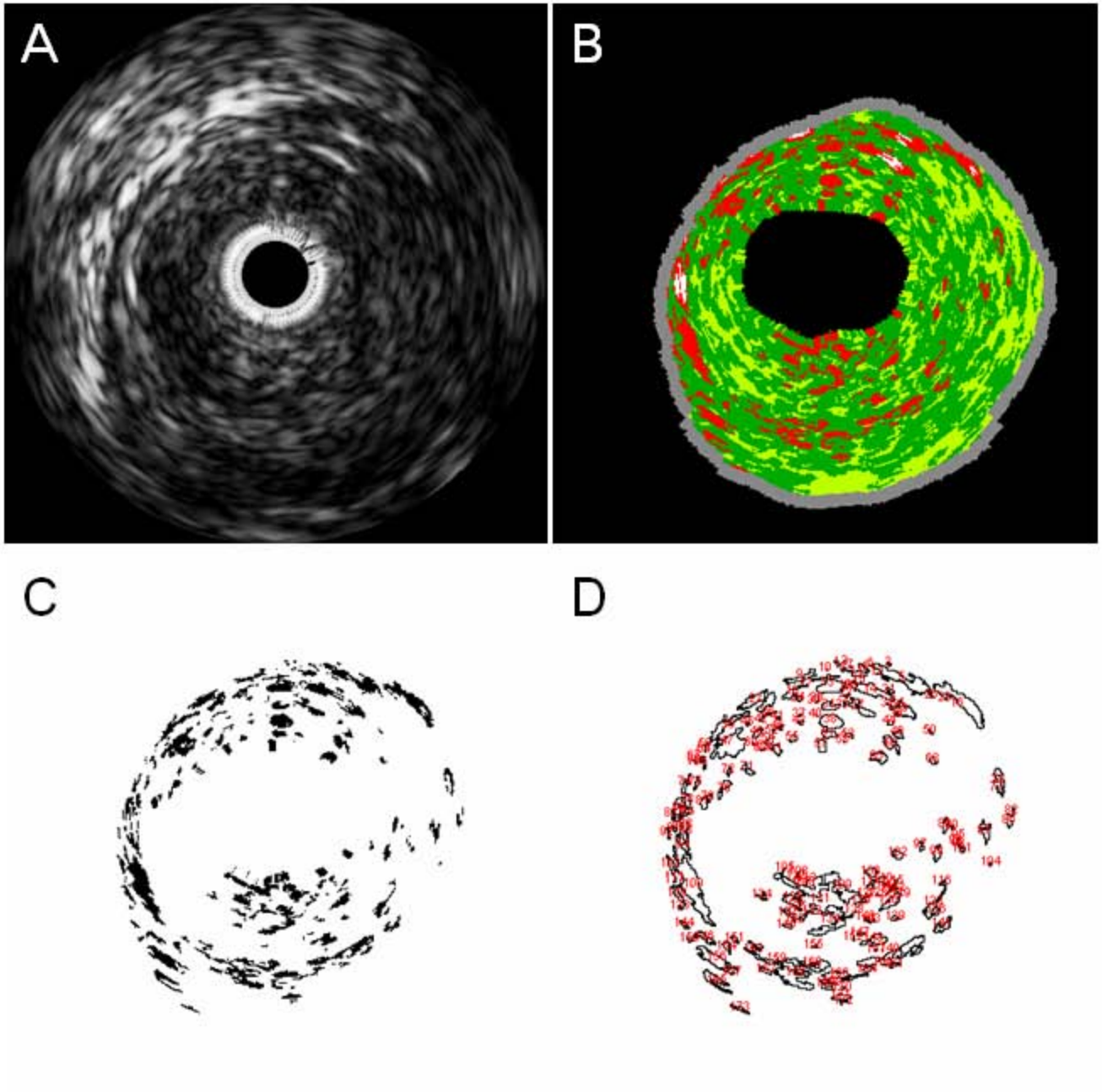

Fig. 2

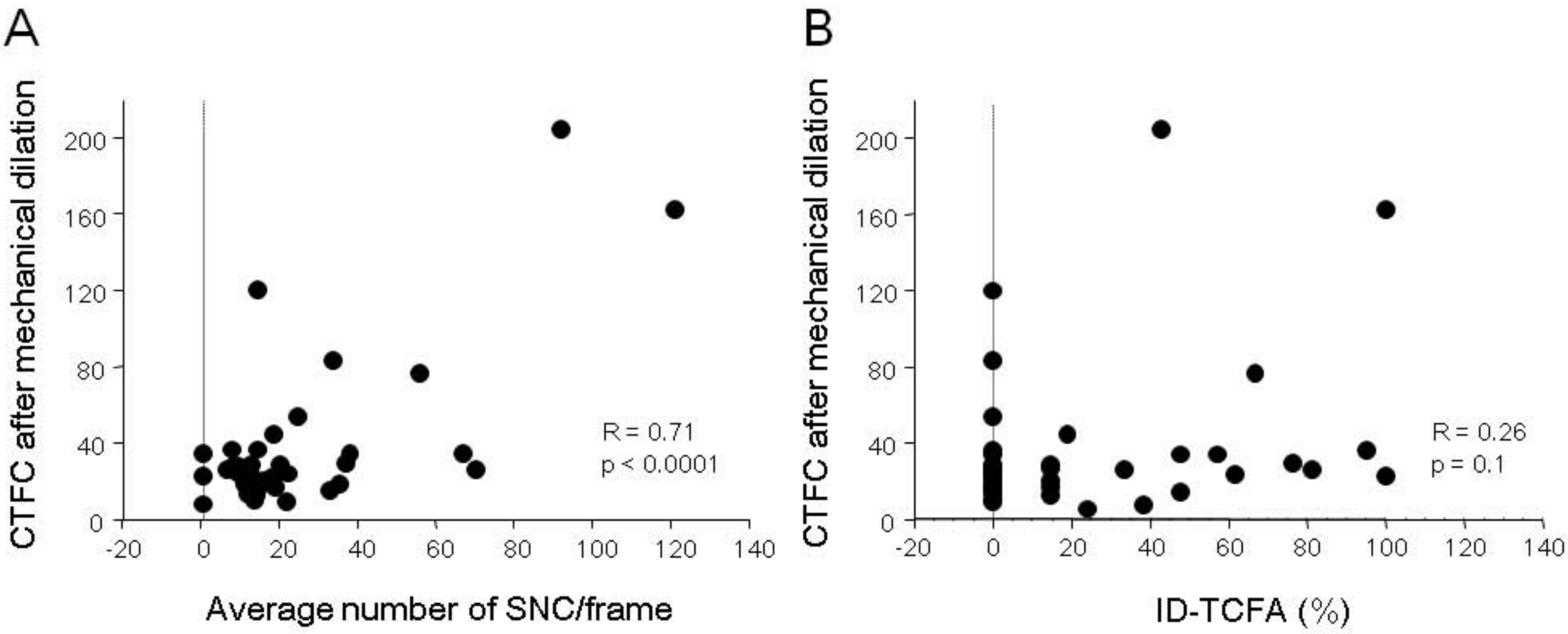
A
CTFC after mechanical dilation
200
160
120
80
40
0
-20
0
20
40
60
80
100
120
140
Average number of SNC/frame
R = 0.71
p < 0.0001
B
CTFC after mechanical dilation
200
160
120
80
40
0
-20
0
20
40
60
80
100
120
140
ID-TCFA (%)
R = 0.26
p = 0.1

Fig. 3

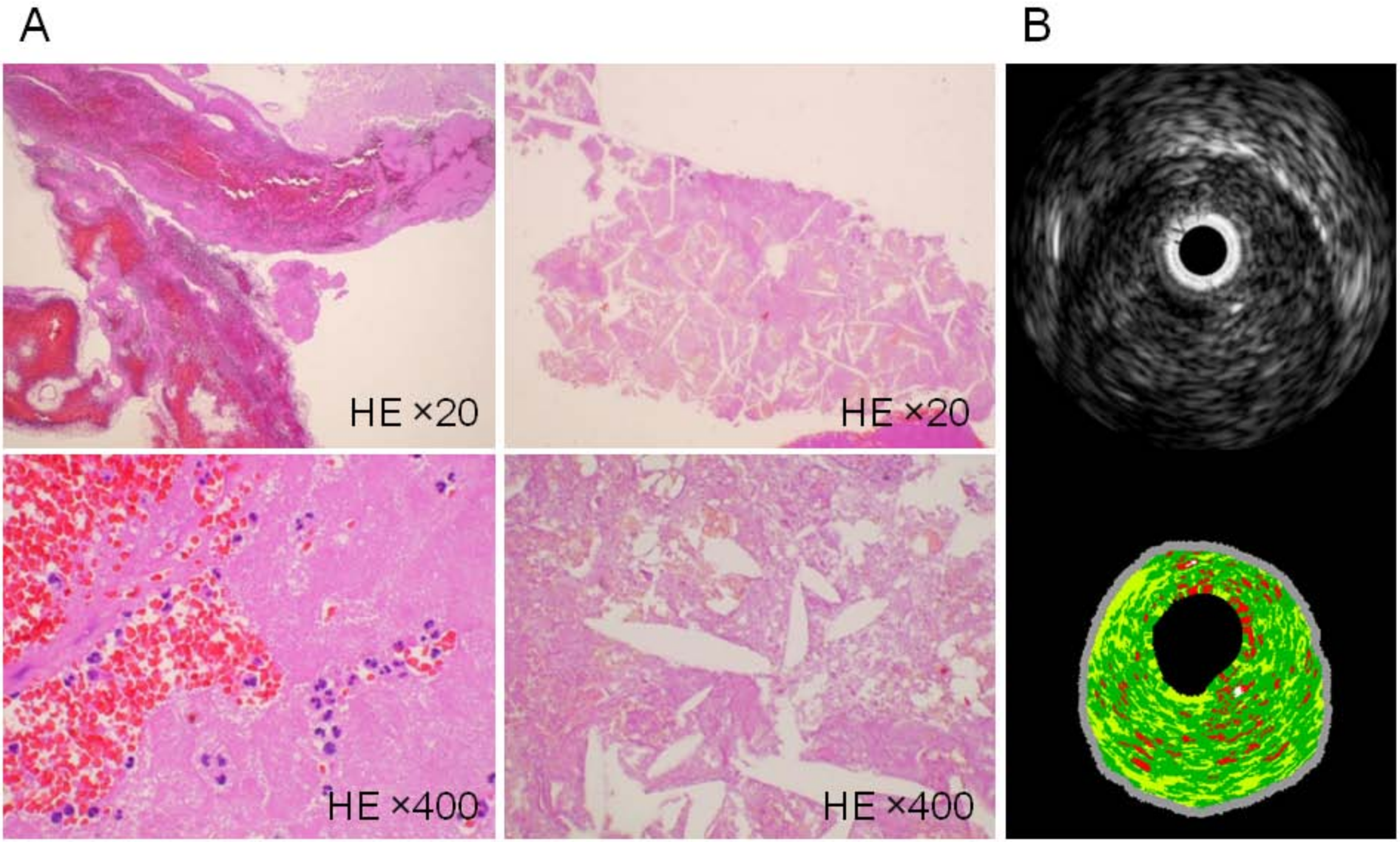

Fig. 4

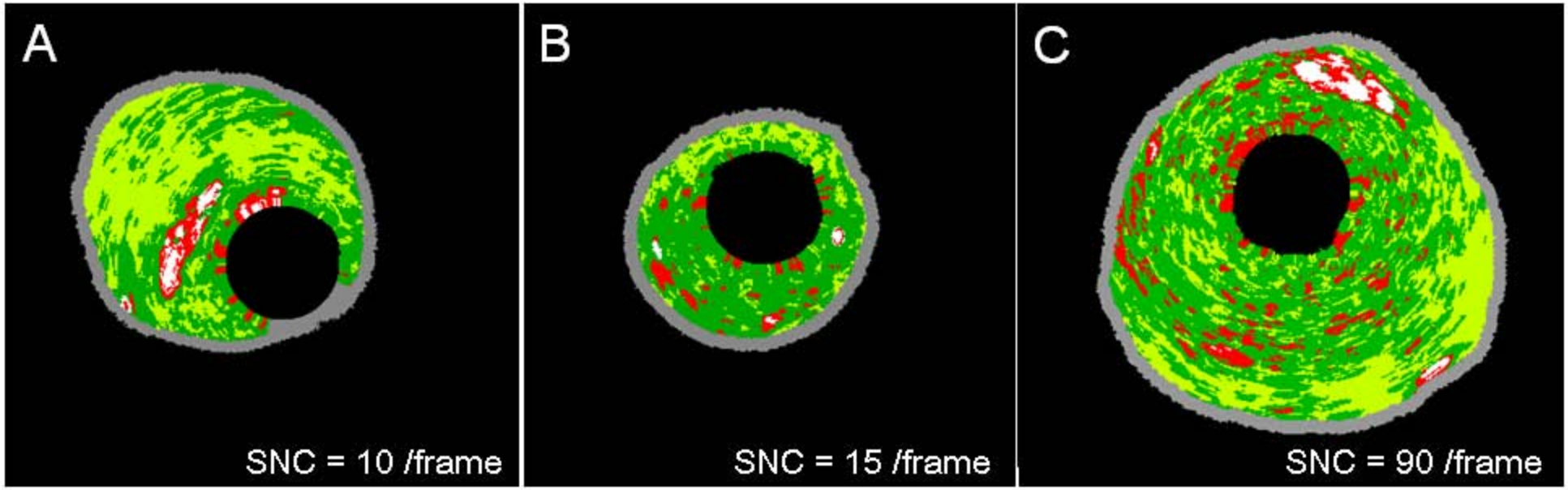

**Table 1. Baseline Characteristics**

| | Coronary flow deterioration Group (n=15) | Normal reflow Group (n=23) | *P* Value |
|---|---|---|---|
| Male | 13 (86.7) | 17 (73.9) | 0.35 |
| Age (years) | 59.9 ± 15.1 | 69.8 ± 11.2 | 0.0259 |
| Systolic BP (mmHg) | 137.7 ± 22.4 | 134.7 ± 22.5 | 0.71 |
| Diastolic BP (mmHg) | 71.8 ± 13.0 | 74.8 ± 13.3 | 0.55 |
| Heart rate (bpm) | 77.3 ± 13.4 | 79.7 ± 13.3 | 0.64 |
| Ejection fraction (%) | 47.0 ± 11.3 | 45.0 ± 8.4 | 0.57 |
| Systemic hypertension | 7 (46.7) | 15 (65.2) | 0.26 |
| Diabetes mellitus | 4 (26.7) | 9 (39.1) | 0.43 |
| Hypercholesterolemia | 5 (33.3) | 7 (30.4) | 0.85 |
| Current smoker | 6 (40.0) | 4 (17.4) | 0.11 |
| Diagnosis | | | 0.19 |
| STEMI | 11 (73.3) | 10 (43.5) | |
| NSTEMI | 1 (6.7) | 4 (17.4) | |
| UAP | 3 (20.0) | 9 (39.1) | |
| Previous angina pectoris | 2 (13.3) | 4 (17.4) | 0.74 |
| Previous MI | 1 (6.7) | 3 (13.0) | 0.53 |
| Reperfusion time (h) | 8.1 ± 5.2 | 6.0 ± 2.0 | 0.16 |
| Target coronary artery | | | |
| LAD/LCX/RCA | 9/0/6 | 13/4/6 | 0.20 |
| Initial TIMI flow grade | | | 0.20 |
| 0/1/2 | 8/3/3 | 6/3/8 | |
| 3 | 1 | 6 | |
| Pre-interventional QCA | | | |
| Lesion length (mm) | 15.5 ± 7.7 | 14.8 ± 6.9 | 0.78 |
| Reference diameter (mm) | 2.6 ± 0.6 | 2.3 ± 0.8 | 0.20 |
| Minimal lumen diameter (mm) | 0.2 ± 0.4 | 0.3 ± 0.4 | 0.51 |
| Diameter stenosis (%) | 91.3 ± 12.9 | 86.7 ± 16.0 | 0.36 |
| PCI procedure | | | |
| Direct stent | 5 (33.3) | 6 (26.1) | 0.63 |
| POBA alone | 3 (20.0) | 1 (4.3) | 0.12 |

| | | | |
|---|---|---|---|
| POBA + stent | 7 (46.7) | 16 (69.6) | 0.16 |
| Max dilation pressure (atm) | 14.9 ± 3.0 | 16.1 ± 3.2 | 0.25 |
| Final balloon or stent size (mm) | 3.5 ± 0.7 | 3.3 ± 0.6 | 0.34 |
| Total stent length (mm) | 21.2 ± 7.4 | 26.2 ± 12.6 | 0.23 |
| Balloon/artery ratio | 1.4 ± 0.4 | 1.6 ± 0.6 | 0.27 |
| Post-interventional QCA | | | |
| Minimal lumen diameter (mm) | 2.7 ± 0.6 | 2.4 ± 0.6 | 0.21 |
| Diameter stenosis (%) | 10.4 ± 14.8 | 11.0 ± 10.0 | 0.88 |
| Final TIMI flow grade 3 | 10 (66.7) | 23 (100) | 0.003 |
| Corrected TIMI frame count after thrombectomy | 32.6 ± 18.3 | 38.1 ± 28.4 | 0.52 |
| Corrected TIMI frame count after mechanical dilation | 65.1 ± 56.2 | 20.3 ± 8.1 | 0.0006 |

Data presented are mean values ± SD or a number (%) of patients.

BP, blood pressure; LAD, left anterior descending; LCX, left circumflex; Max, maximum; MI, myocardial infarction; NSTEMI, non ST-segment elevation myocardial infarction; PCI, percutaneous coronary intervention; POBA, plain old balloon angioplasty; QCA, quantitative coronary angiography; RCA, right coronary artery; SD, standard deviation; STEMI, ST-segment elevation myocardial infarction; TIMI, Thrombolysis In Myocardial Infarction; UAP, unstable angina pectoris.

## Table 2. Conventional Intravascular Ultrasound Analysis

| | Coronary flow deterioration Group (n=15) | Normal reflow Group (n=23) | *P* Value |
|---|---|---|---|
| Proximal reference | | | |
| EEM CSA ($mm^2$) | 20.2 ± 6.0 | 18.1 ± 6.3 | 0.32 |
| Lumen CSA ($mm^2$) | 8.0 ± 3.6 | 7.9 ± 4.0 | 0.91 |
| Plaque & media CSA ($mm^2$) | 11.4 ± 5.6 | 10.2 ± 3.5 | 0.43 |
| Minimal lumen site | | | |
| EEM CSA ($mm^2$) | 19.6 ± 8.4 | 16.0 ± 5.6 | 0.13 |
| Lumen CSA ($mm^2$) | 3.0 ± 0.5 | 3.1 ± 1.2 | 0.91 |
| Plaque & media CSA ($mm^2$) | 15.5 ± 9.0 | 12.9 ± 4.9 | 0.27 |
| Plaque burden (%) | 82.2 ± 7.3 | 79.9 ± 6.0 | 0.32 |
| Remodeling index | 1.0 ± 0.2 | 0.9 ± 0.2 | 0.30 |
| Positive remodeling (%) | 5 (33.3) | 6 (26.1) | 0.63 |
| Distal reference | | | |
| EEM CSA ($mm^2$) | 14.4 ± 5.8 | 13.3 ± 5.6 | 0.57 |
| Lumen CSA ($mm^2$) | 7.0 ± 3.7 | 6.2 ± 3.4 | 0.56 |
| Plaque & media CSA ($mm^2$) | 7.4 ± 3.5 | 7.0 ± 3.4 | 0.73 |
| Volumetric analysis | | | |
| EEM volume ($mm^3$) | 162.2 ± 51.5 | 119.9 ± 55.2 | 0.0292 |
| Lumen volume ($mm^3$) | 39.8 ± 13.3 | 35.8 ± 13.3 | 0.39 |
| Plaque & media volume ($mm^3$) | 122.4 ± 49.8 | 91.5 ± 38.4 | 0.0494 |
| Qualitative analysis | | | |
| Residual thrombus | 11 (73.3) | 7 (30.4) | 0.0096 |
| Plaque rupture | 12 (80.0) | 6 (26.1) | 0.0011 |
| Lipid pool image | 4 (26.7) | 4 (17.4) | 0.49 |
| Spotty calcification | 11 (73.3) | 13 (56.5) | 0.29 |

Data presented are mean values ± SD or a number (%) of patients.

CS, cross sectional area; EEM, external elastic membrane.

**Table 3. Virtual Histology Intravascular Ultrasound Analysis**

| | Coronary flow deterioration Group (n=15) | Normal reflow Group (n=23) | *P* Value |
|---|---|---|---|
| Minimum lumen site | | | |
| Absolute plaque area ($mm^2$) | | | |
| Fibrous | 8.0±4.2 | 5.8±2.4 | 0.0478 |
| Fibrofatty | 2.5±3.0 | 1.4 ±1.8 | 0.19 |
| Dense calcium | 0.6±0.7 | 0.7±0.5 | 0.62 |
| Necrotic core | 2.0±1.3 | 1.9±1.5 | 0.85 |
| Relative plaque area (%) | | | |
| Fibrous | 61.1±12.0 | 59.0±13.4 | 0.64 |
| Fibrofatty | 16.1±14.0 | 12.7±12.1 | 0.42 |
| Dense calcium | 4.1±4.0 | 7.7±7.2 | 0.09 |
| Necrotic core | 18.0±12.4 | 19.5±13.6 | 0.74 |
| Plaque distribution analysis | | | |
| SNC/necrotic core (%) | 9.0±3.9 | 6.1±3.7 | 0.0295 |
| Number of SNC | 71.5±42.8 | 33.3±16.8 | 0.0004 |
| Entire culprit lesion | | | |
| Absolute plaque volume ($mm^3$) | | | |
| Fibrous | 54.9±32.9 | 34.4±20.0 | 0.0318 |
| Fibrofatty | 16.3±18.0 | 7.4 ±9.2 | 0.07 |
| Dense calcium | 3.9±3.2 | 6.3±4.7 | 0.10 |
| Necrotic core | 14.5±8.4 | 13.8±11.5 | 0.86 |
| Relative plaque volume (%) | | | |
| Fibrous | 59.9±10.5 | 56.8±15.3 | 0.51 |
| Fibrofatty | 15.9±13.6 | 11.1±8.5 | 0.22 |
| Dense calcium | 6.5±5.6 | 10.1±7.7 | 0.12 |
| Necrotic core | 17.9±10.4 | 22.1±12.4 | 0.31 |
| Plaque distribution analysis | | | |
| Thin-cap fibroatheroma (%) | 42.5±37.1 | 14.1±24.2 | 0.0068 |
| Max number of SNC/lesion | 76.1±42.4 | 42.6±25.0 | 0.004 |
| SNC/necrotic core (%) | 7.5±3.2 | 6.6±3.8 | 0.48 |
| Average number of SNC/frame | 42.3±32.1 | 12.4±7.7 | 0.0001 |

Data presented are mean values ± SD.

SNC, scattered necrotic core.

**Table 4. Independent Predictors of Coronary Flow Deterioration by Multivariate Logistic Regression Analysis**

| | Odds Ratio | 95% CI | p-value |
|---|---|---|---|
| Age (yrs) | 0.96 | 0.87-1.06 | 0.430 |
| Fibrous volume ($mm^3$/cm) | 1.03 | 0.96-1.10 | 0.458 |
| EEM volume ($mm^3$) | 1.00 | 0.97-1.02 | 0.836 |
| Residual thrombus (%) | 1.64 | 0.17-15.86 | 0.667 |
| Plaque rupture (%) | 1.11 | 0.10-12.14 | 0.933 |
| Thin-cap fibroatheroma (%) | 1.03 | 0.99-1.07 | 0.095 |
| Number of SNC/frame | 1.18 | 1.02-1.37 | 0.023 |

CI: confidence interval; EEM: external elastic membrane; SNC: scattered necrotic core.